Picometer Interferometry and its Application in Dilatometry and Surface Metrology

Thilo Schuldt[1,#], Martin Gohlke[2,3] , Harald Kögel[1,3], Ruven Spannagel[1] ,Achim Peters[2], Ulrich Johann[3], Dennis Weise[3] and Claus Braxmaier[1,3]

1 Hochschule für Technik, Wirtschaft und Gestaltung (HTWG) Konstanz, Brauneggerstr. 55, 78462 Konstanz, Germany
2 Humboldt-Universität zu Berlin, Newtonstr. 15, 12489 Berlin, Germany
3 Astrium GmbH – Satellites, Claude-Dornier-Straße, 88090 Immenstaad, Germany
Corresponding Author / E-mail: tschuldt@htwg-konstanz.de, TEL: +49-7531-206-379, FAX: +49-7531-206-521

KEYWORDS : Optical metrology, Heterodyne Interferometry, Dilatometry, Surface Metrology

A high-sensitivity heterodyne interferometer implementing differential wavefront sensing (DWS) for tilt measurement was developed over the last years where noise levels below 5 pm/√Hz in translation measurement and below 10 nrad/√Hz in tilt measurement, both for frequencies above 10^{-2} Hz, were demonstrated in laboratory experiments. These results were obtained with a prototype setup using an aluminum breadboard and compact optical mounts with a beam height of 2 cm. Here, we present a new compact and ruggedized interferometer setup utilizing a baseplate made of Zerodur, a thermally and mechanically highly stable glass ceramics with a coefficient of thermal expansion (CTE) of $2 \cdot 10^{-8}$ K^{-1}. The optical components are fixed to the baseplate using a specifically developed easy-to-handle assembly-integration technology based on a space-qualified two-component epoxy. Beside its potential future application aboard satellite space missions (such as LISA, Laser Interferometer Space Antenna), the interferometer is used in laboratory experiments for dilatometry and surface metrology. A first dilatometer setup with a demonstrated accuracy of 10^{-7} K^{-1} in CTE measurement was realized. As it was seen that the accuracy is limited by the dimensional stability of the sample tube support, a new setup was developed utilizing Zerodur as structural material for the sample tube support. In another activity, the interferometer is used for characterization of high quality mirror surfaces at the picometer level and for high-accuracy two-dimensional surface characterization in a prototype for industrial applications. In this paper, the corresponding designs, their realizations and first measurements of both applications in dilatometry and surface metrology are presented.

Manuscript received: January XX, 2011 / Accepted: January XX, 2011

NOMENCLATURE

f_1 = frequency of the first laser beam
f_2 = frequency of the second laser beam
f_{het} = heterodyne frequency
CTE = coefficient of thermal expansion
ΔT = change in temperature
ΔL = change in distance L
L = distance between measurement and reference mirror

1. Introduction

Optical interferometry represents the basis for various measurements e.g. in position metrology, surface characterization, actuator verification and dimensional characterization of highly stable materials. It offers highest sensitivity and accuracy while providing a non-tactile measurement method. Interferometers exist in a variety of different implementations and can be subdivided in homodyne (use of one laser frequency) and heterodyne (use of two laser frequencies) interferometers where heterodyne interferometers have a potential higher performance due to higher noise immunity, especially with respect to DC light intensity variations at the detector, e.g. caused by straylight influence.

Over the last years a highly-symmetric heterodyne interferometer was developed in a collaboration of the University of Applied Sciences Konstanz, the European space company Astrium GmbH (Friedrichshafen) and the Humboldt-University Berlin. It serves as a prototype for a possible optical readout aboard the LISA (Laser Interferometer Space Antenna) satellites where changes in translation and tilt of a free floating test mass with respect to the its housing must be measured with ~1 pm/√Hz and 20 nrad/√Hz sensitivity [1]. This development was later on the basis for a much broader investigation of interferometric measurement techniques in the laboratory: An optical dilatometer setup for characterizing ultra-low expansion materials such as carbon-fiber reinforced plastic (CFRP) or glass ceramics such as Zerodur or ULE was developed [2,3]. The interferometer was utilized for characterization of high precision

actuators such as the commercially available piezo stepper Nexline by PI GmbH and a specifically designed tilt-actuated micromirror which was developed in collaboration with the University of Applied Sciences Furtwangen [4]. A setup for characterizing surfaces as a prototype for industrial metrology [5] and a specific setup for high-accuracy characterization of high-reflectivity mirror surfaces were realized.

In the following, an overview over the interferometer setup and its new quasi-monolithic implementation as well as its application in dilatometry and profilometry will be given.

2. Heterodyne Interferometer

The heterodyne interferometer is based on a highly symmetric design where measurement and reference beam have the same frequency and polarization and similar optical pathlengths [6,7]. Frequency and polarization mixing is therefore avoided. For tilt measurement, the method of differential wavefront sensing (DWS, [8,9]) is implemented. The setup for heterodyne frequency generation, the interferometer setup and the digital phase measurement are detailed in the following. The advanced quasi-monolithic interferometer setup using ultra-low expansion glass material for the baseplate is described.

2.1 Heterodyne Frequency Generation

For generating two spatially separated laser beams with different frequencies f_1 and f_2, the laser light is split and each laser beam is shifted in frequency using an acousto-optical modulator (AOM). As laser source a non-planar ring-oscillator (NPRO) Nd:YAG laser with a wavelength of 1064 nm is used. This type of laser guarantees an intrinsically very high intensity and frequency stability. The RF driving frequencies of the two AOMs are 79.99 MHz and 80.00 MHz, respectively – resulting in a heterodyne frequency of 10 kHz. The RF frequencies are generated using two phase locked direct digital synthesizers (DDS). Both laser beams are fiber-coupled and sent to the interferometer board, which is placed in a vacuum chamber and operated at pressures below 10^{-3} mbar.

2.2 Interferometer Setup

The compact interferometer is set up on an 440 mm x 300 mm x 40 mm aluminum board using specifically designed optical mounts with a beam height of only 2 cm, cf. Fig.1. The laser beams have a diameter of ~1.4 mm and output powers of about 0.5 mW at fiber output. Polarizers after fiber outcoupling ensure linear and proper polarization. At a glass plate, part of each beam is split off and directed on a power monitoring photo detector (PD1 and PD2 in Fig.1). Additionally, part of each laser beam is overlapped on a third photo detector (PD3). This signal at the heterodyne frequency is phase compared to an electronically generated reference signal also at f_{het}. Using a PZT-mounted mirror in front of the fiber-coupling outside the vacuum chamber, the phase of the signal detected by PD3 is phase locked to the reference signal – therefore minimizing differential phase effects caused by the fibers and the AOMs. This phase lock was seen to be crucial to get down to a noise floor of a few pm [1]. The laser beams used in the interferometer are both split into two parallel laser beams using symmetric beamsplitters. The laser beams with frequency f_1 (marked red in Fig.1) are reflected at a polarizing beamsplitter (PBS) towards measurement and reference mirror. One beam represents the measurement beam, the other the reference beam of the interferometer. After passing twice a $\lambda/4$ waveplate, both beams are transmitted at the PBS and overlapped with the laser beams with frequency f_2 (marked blue in Fig.1) at a non-polarizing beamsplitter. Two silicon quadrant photo detectors provide the measurement signal (QPD1) and the reference signal (QPD2). The optical powers are ~100 μW at the photo detectors.

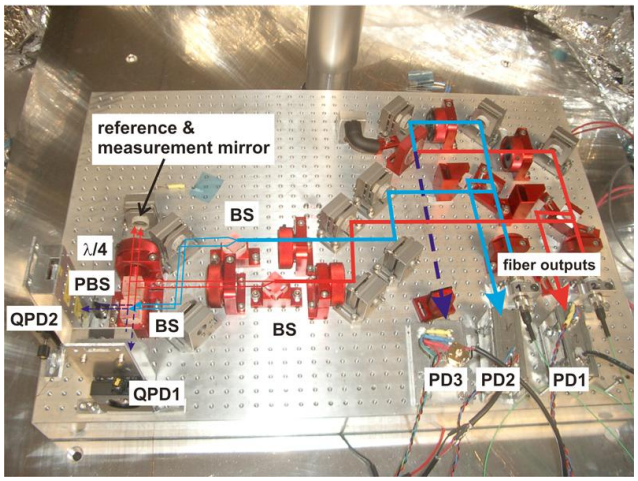

Fig. 1 Photograph of the interferometer setup using an aluminum baseplate with schematic of the optical path. The two frequencies are fiber-coupled to the interferometer board (PBS: polarizing beamsplitter; BS: beamsplitter, PD: photodiode; QPD: quadrant photodiode). For noise measurement, reference and measurement mirror are represented by one fixed mirror.

2.3 Phase Measurement

Each of the two quadrant photodiodes delivers four signals at the heterodyne frequency of 10 kHz, representing the single quadrants. All signals are pre-amplified and anti-aliasing filtered; they are simultaneously digitized using a field programmable gate array (FPGA) board by National Instruments programmed with LabVIEW. On the FPGA, a digital phasemeter is implemented. Each signal is compared in phase relative to an internally generated 10 kHz reference signal. By processing the appropriate signals, the translation of the measurement mirror and the tilt of measurement and reference mirror are calculated. The LabVIEW program also includes an in-quadrature measurement of the phases.

2.4 Advanced Interferometer Setup

Based on the design of the aluminum breadboard interferometer as detailed above, an advanced, more compact and mechanically and thermally highly stable interferometer design was developed and realized, cf. Fig. 2. The baseplate is made of Zerodur, a glass ceramics with a very low CTE of $2 \cdot 10^{-8}$ K^{-1} where the optical components are fixed to the baseplate using adhesive patching technology. This assembly-integration (AI) technology was specifically developed and evaluated with respect to space application [10]. Compared to hydroxide-catalysis bonding technology [11], which represents the standard state-of-the-art AI-technology for high-stability optical space systems, adhesive patching offers the advantages of a much longer adjustment time (up to several hours) and no need of clean room environment.

The design of the quadrant photo detectors is adapted to the LISA requirement where the detected heterodyne frequency is varying between 2 to 20 MHz caused by a relative movement of the three

spacecraft. The detector therefore utilizes InGaAs photodiodes with a responsivity of 0.7 A/W at 1064 nm in combination with MHz electronics. The electronics implements an AC-path (2 to 20 MHz) and a DC-path (up to 30 kHz); the maximum optical power is 1 mW.

The noise performance of the new interferometer in combination with advanced photo detectors and phase measurement is currently under way.

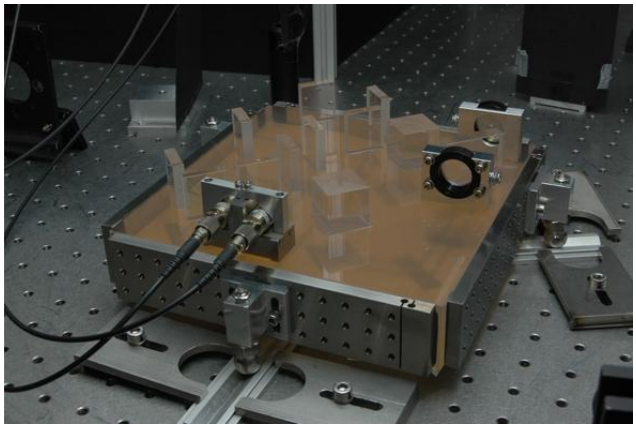

Fig. 2 Photograph of the integrated interferometer. The optical components are connected to a Zerodur baseplate using adhesive patching technology.

3. Dilatometry

The interferometer as described before is the basis for a setup for measuring the linear coefficient of thermal expansion (CTE) of thermally and mechanically highly stable materials. The principle of the CTE measurement is shown in Fig. 3. Reference and measurement mirror are fixed inside a tube made of the material under investigation. The tube is placed inside a Peltier heating where a change in temperature (ΔT) of the tube causes an expansion (or contraction, ΔL) of the tube. This change in distance between the two mirrors is measured with sub-nanometer sensitivity using the heterodyne interferometer.

A first setup is realized using a tube support made of aluminum and thin-walled fibreglass tubes. Three fine-thread screws allow for the angular adjustment of the tube relative to measurement and reference beams of the interferometer. The mirror clamps fixing the mirrors inside the tube are specifically designed in order not to influence the CTE measurement. The clamps are made of Invar, a material with a low CTE of $< 10^{-6}$ K^{-1}. Each clamp has six legs of the same length; three of them fix the mirror inside the clamp, the other three fix the clamp inside the tube. The reflective mirror surface together with the six clamping points of the clamp legs define a thermally neutral plane, which in case of a thermal expansion of the clamp keeps the reflective mirror surface unmoved (cf. the schematics in Fig. 5, right).

First measurements were carried out with a CFRP (carbon-fiber reinforced plastics) tube with known CTE. Different temperature variations, such as sine and square wave functions, were applied to the temperature controller and measurements with different offset temperatures, amplitudes and frequencies were carried out. The CTE is calculated via:

$$CTE = \frac{1}{L} \cdot \frac{\Delta L}{\Delta T},$$

where ΔL is obtained by the interferometer measurement, ΔT by use of high-sensitivity Pt-100 temperature sensors glued to the sample tube and L using a mechanical gauge. Different evaluation methods, such as hysteresis evaluation, frequency analysis and least square sine fit, were applied to the measurement data. The obtained CTE value of $(-0.6 \pm 0.1)\cdot 10^{-6}$ K^{-1} agrees with the theoretically determined value of $-0.647\cdot 10^{-6}$ K^{-1}. A typical measurement with sine thermal cycling and a period of 1 h is shown in Fig. 4. The temperature was varied by about ±3.1 K at an offset temperature of 30°C. As a tilt of the measurement and reference mirror implies an unwanted change in pathlength, the DWS signals of both mirrors are taken for correction of the translation signal.

With this setup, it was seen that the main limitation in CTE measurement is the stability of the sample tube support under thermal load where the sample tube is tilted with respect to the interferometer beams. Therefore, a new support was designed and realized using Zerodur as structural material, cf. Fig. 5. A first measurement of a CFRP tube with an intended CTE $<< 10^{-7}$ K^{-1} is shown in Fig. 6. The short-term perturbations in the translation measurement are caused by laser frequency noise. This noise contribution was measured by beating the laser used in the interferometer with a laser frequency stabilized to a ULE cavity. The measured frequency variations were used for correction of the interferometric translation signal (cf. Fig. 6). The measured CTE is $(-2.17 \pm 0.24)\cdot 10^{-6}$ K^{-1}.

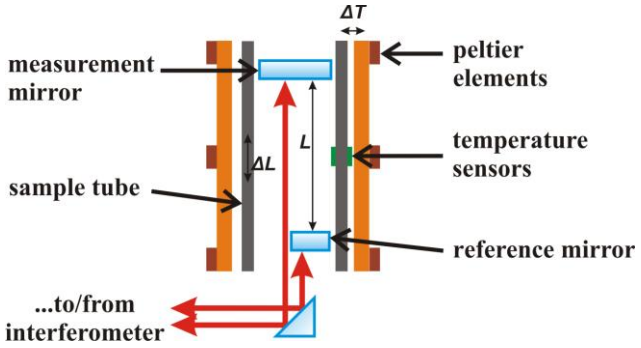

Fig. 3 Sketch of the dilatometer setup [2]. Two mirrors are fixed inside the tube made of the material under investigation. The interferometer measures changes in distance between the two mirrors with nm-sensitivity while applying a thermal load to the sample tube.

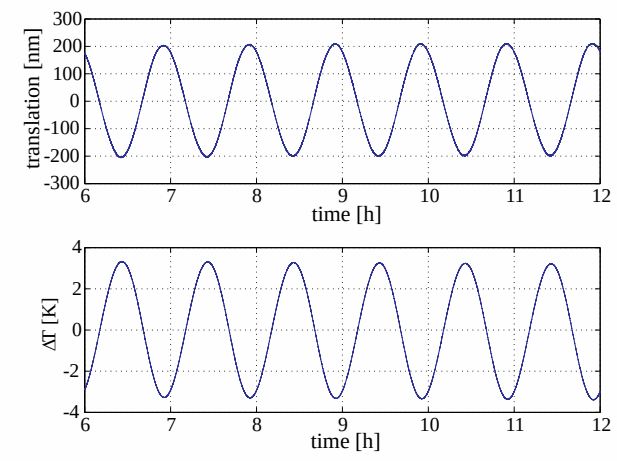

Fig. 4 Typical measurement for CTE evaluation. A sine thermal cycling with a period of 1 h is applied to a sample tube made of CFRP. A change in temperature of about ±3.1°C measured at the tube results in a change of length of the tube of about 400 nm.

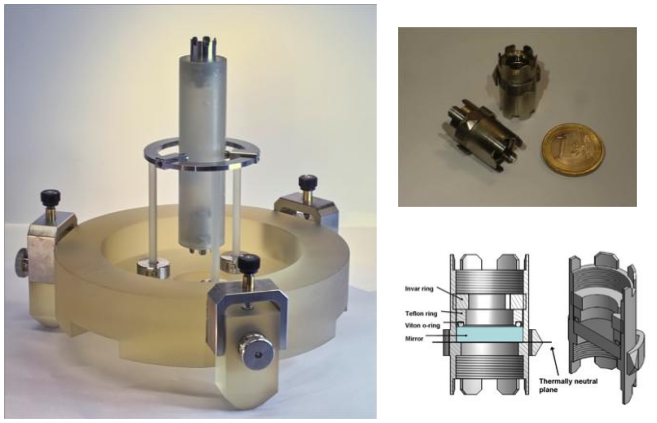

Fig. 5 Photograph of the highly-stable sample tube holder for dilatometry, made of Zerodur (left). Here, a sample tube made of Zerodur is mounted for CTE evaluation; the mirror mounts are clamped inside the tube. A photograph and a schematic of the mirror mounts made of Invar are shown to the right.

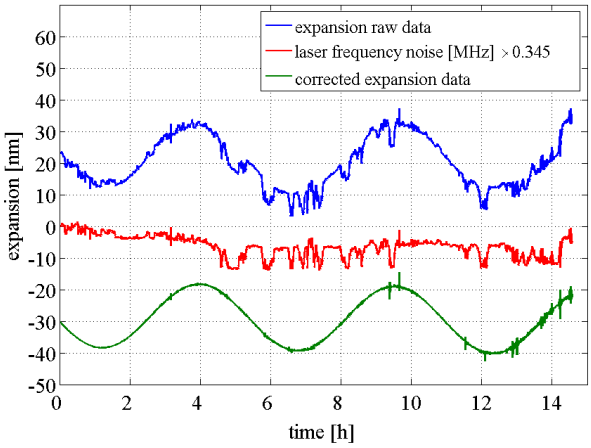

Fig. 6 Expansion measurement of a CFRP tube specifically designed to have a CTE << 10^{-7} K^{-1}. The original translation measurement of the interferometer is shown at the top (blue curve). The short term perturbations are caused by laser frequency noise (compare middle/red curve). The lower (green) line represents the translation signal corrected by the influence of laser frequency noise.

4. Surface Metrology

With the interferometer design described in chapter 2, translation and tilt of a measurement mirror at one single spot can be measured with high sensitivity. For surface characterization, a scan of the measurement beam over the surface under investigation is necessary which can either be realized by actuating the device under test (DUT) or the measurement beam of the interferometer. Two setups with different goals were developed: One is a prototype for industrial metrology with focus on compactness and simplicity but with nanometer resolution. The other one is a prototype for characterizing high-reflectivity mirrors with sub-nanometer resolution. This is also of interest for the LISA space mission where actuated mirrors are needed on the optical bench. During actuation, the laser beam reflected at the actuated mirror is scanned over mirror surfaces in its subsequent optical path. In case of LISA it has to be verified, that the optical pathlength can be reproducibly controlled at the picometer level.

A photograph of the prototype for industrial metrology is shown in Fig. 7. The optical layout is based on the interferometer as detailed in chapter 2. For surface scanning, two concepts were investigated: (i) implementation of an xy-PZT translation stage actuating the DUT perpendicularly to the measurement beam of the interferometer, and (ii) implementation of an actuation of the measurement beam using two Dove prisms. It was seen, that the setup with sample actuation yields to lower noise levels; also the adjustment is easier due to less DOFs. With this setup an accuracy of about 5 nm was achieved. The lateral resolution was approximately 15µm using a lens with a focal length of 15 mm focusing the measurement beam on the DUT surface. The functionality of the setup was verified by measuring a reference surface with a known grating structure (cf. Fig. 8).

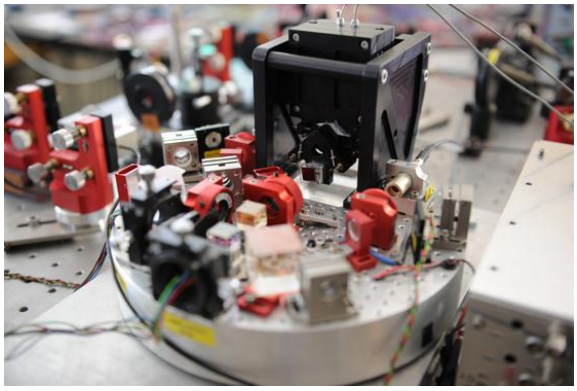

Fig. 7 Photograph of the prototype interferometer for industrial metrology. An xy-PZT translation stage is implemented performing a scan of the surface under investigation.

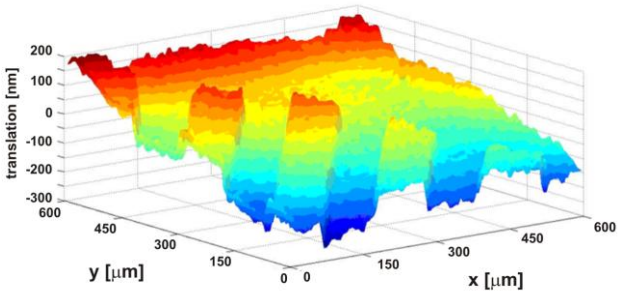

Fig. 8 Surface scan of a reference surface (grating) with 200 µm pitch and a height of 90 nm.

For the characterization of high-reflectivity mirror surfaces a specific pendulum was developed, as shown in Fig. 9. It ensures a high-precision actuation of the two mirrors under investigation perpendicularly to measurement and reference beam of the interferometer. A commercially available PZT-stepper (Nexline by PI GmbH) was used for actuation, where a stepped triangle function is applied to the pendulum. The step size is 10 µm, the total actuation range 2000 µm. The measurement was repeated three times and the translation recorded for up-and-down line. The measured statistical spread between the measurements is below 0.2 nm. The two mirrors under investigation are mounted to the lower end of the pendulum, where both mirror surfaces are pressed against the same glass plate with high planeness in order to guarantee the parallelism of the two reflected laser beams. In a first measurement both, measurement and reference laser beam of the interferometer, are reflected on the same mirror in the pendulum. The corresponding measured differential translation is shown in Fig. 10. The large beam diameter on the mirror (~1.3 mm) limit the lateral resolution.

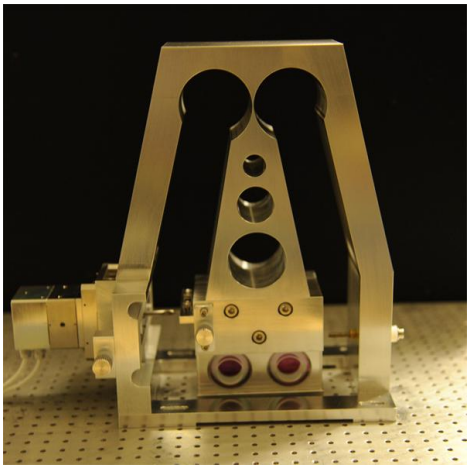

Fig. 9 Photograph of the aluminum pendulum for characterizing mirror surfaces at the sub-nanometer level. Measurement and reference beam of the interferometer are reflected at two mirrors mounted at the bottom of the pendulum. The mirrors are actuated perpendicularly to the laser beams using a PI Nexline piezo stepper.

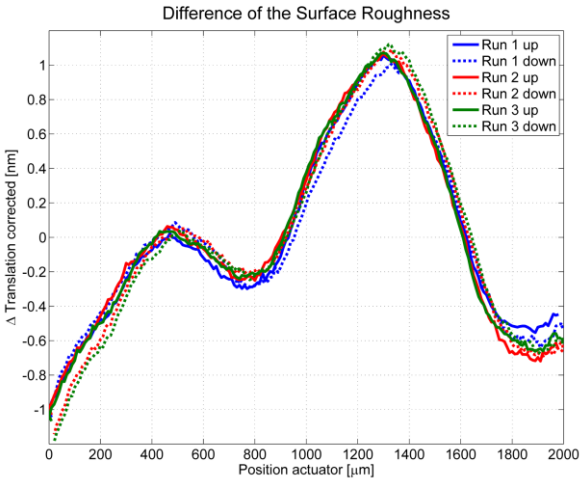

Fig. 10 Measurement showing the difference of the surface roughness measured on one mirror, which is actuated with a step size of 10 µm over a total distance of 2000 µm.

5. Conclusions

We presented the current status of our heterodyne interferometer development with focus on an advanced setup using thermally and mechanically highly stable glass ceramics as baseplate material in combination with a specifically developed assembly-integration technology. This interferometer serves as a demonstrator for a possible optical readout for the LISA gravitational reference sensor where pm- and nrad-sensitivity is shown in experiment. Beside that, the interferometer setup is used for applications in dilatometry and profilometry. In dilatometry, up to now, an accuracy of 10^{-7} K^{-1} in CTE measurement is achieved with potential to further reach 10^{-8} K^{-1} accuracy. A first profilometer setup for industrial metrology was realized and verified by measuring a reference grating. An accuracy of approximately 5 nm was demonstrated. First measurements were carried out with a setup for characterizing high-reflectivity mirrors. Here, a sub-nm reproducibility was shown.

ACKNOWLEDGEMENT

Financial support by the European Union under European Funds for Regional Development (EFRE) and the State Baden-Württemberg within the program ZAFH 'Photon^{n}' and the German Aerospace Center (Deutsches Zentrum für Luft- und Raumfahrt, DLR) within the program 'LISA Performance Engineering' (DLR contract number 50OQ0701) is highly appreciated.

REFERENCES

1. Schuldt, T., Gohlke, M., Weise, D., Johann, U., Peters, A., Braxmaier, C., 'Picometer and nanoradian optical heterodyne interferometry for translation and tilt metrology of the LISA gravitational reference sensor,' Class. Quantum Grav. 26, 085008, 2009
2. Cordero, J., Heinrich, T., Schuldt, T., Gohlke, M., Lucarelli, S., Weise, D., Johann, U., Braxmaier, C., 'Interferometry based high-precision dilatometry for dimensional characterization of highly stable materials,' Meas. Sci. Technol. 20, 095301, 2009
3. Schuldt, T., Gohlke, M., Weise, D., Johann, U., Braxmaier, C., 'A high-precision dilatometer based on sub-nm heterodyne interferometry,' IEEE Conf. Proc. (ISOT 2009), 146-151
4. Kronast, W., Mescheder, U., Müller, B., Nimo, A., Braxmaier, C., Schuldt, T., ' Development of a tilt-actuated micromirror for applications in laser interferometry,' Proc. SPIE, Vol 7594, MOEMS and miniaturized systems IX, 759400 (2010)
5. Schuldt, T., Gohlke, M., Spannagel, R., Ressel, S., Weise, D., Johann, U., Braxmaier, C., 'Sub-nanometer heterodyne interferometry and its application in dilatometry and industrial metrology,' Int. J. Optomechatronics, 3:187-200, 2009
6. Wu, C., 'Periodic nonlinearity resulting from ghost reflections in heterodyne interferometry,' Opt. Commun. 215(13):17-23
7. Wu, C., Lin, S., Fu, J., 'Heterodyne interferometer with two spatial-separated polarization beams for nanometrology,' Opt. Quantum Electron. 34(12):1267-1276
8. Morrison, E., Meers, B. J., Robertson, D. I., Ward, H., 'Automatic alignment of optical interferometers,' Appl. Opt. 33(22):5041-5049
9. Morrison, E., Meers, B. J., Robertson, D. I., Ward, H., 'Experimental demonstration of an automatic alignment system for optical interferometers,' Appl. Opt. 33(22):5037-5040
10. Ressel, S., Gohlke, M., Rauen, D., Schuldt, T., Kronast, W., Mescheder, U., Johann, U., Weise, D., Braxmaier, C., 'Ultrastable assembly and integration technology for ground- and space-based optical systems, Appl. Opt. 49(22):4296-4303, 2010
11. Ellife, E. J., Bogenstahl, J., Geshpande, A., Hough, J., Killow, C., Reid, S., Robertson, D., Rowan, S., Ward, H., Cagnoli, G., 'Hydroxide-catalysis bonding for stable optical systems for space,' Class. Quantum Grav. 22, S257-S267, 2005